

Numerical analysis of formation and evolution of global strings in $2 + 1$ dimensions

Masahide Yamaguchi

*Department of Physics, University of Tokyo,
Tokyo, 113-0033, Japan*

Jun'ichi Yokoyama

*Department of Physics, Stanford University,
Stanford, CA 94305-4060, USA
and Yukawa Institute for Theoretical Physics, Kyoto University,
Kyoto, 606-8502, Japan*

M. Kawasaki

*Institute for Cosmic Ray Research, University of Tokyo,
Tokyo, 188-8502, Japan*

Abstract

We simulate the formation and the evolution of global strings taking into account the expansion of the universe and the concomitant change of the effective potential, that is, the change from the restoration stage of the global $U(1)$ -symmetry to the broken stage. Starting from the thermal equilibrium state, we run simulations for 100 sets of different initial conditions in $2+1$ dimensions. As a result, we find deviation from scale invariance. This is because the energy loss mechanism is pair annihilation rather than intercommutation, so that a string and an anti-string attract each other under a logarithmic potential.

1 Introduction

Since the possibility of the restoration of broken symmetries in the very early universe was suggested [1], the cosmological consequences of the accompanying phase transitions have been investigated by a number of authors [2]. As Kibble first pointed out, topological defects of various types may be formed, depending on the pattern of the symmetry breaking [3] (see also Ref. [4] for review). If the symmetry group G breaks into a subgroup H and the coset space G/H is not simply-connected, strings are formed. Strings as local defects have been extensively investigated in the context of structure formation theory [5]. On the other hand, global strings are predicted in the axion theory of the strong CP problem [6], and they may have radiated significant amount of axions as the universe cools down from the Peccei-Quinn breaking scale to the energy scale of QCD [7]. Also, in condensed-matter systems, analogous vortices are observed [8].

Most studies of the formation of strings have employed Monte-Carlo simulations. Vachaspati and Vilenkin [9] first examined the initial configuration of a string network. They found that it has the statistical properties of a Brownian random walk (see also Ref. [10]), and found that a string network is made of closed loops with a scale-invariant size distribution and infinite strings occupying 80% of the total string length. Since that time, many authors have reexamined the problem in more realistic situations than the original, focusing especially on the existence and the fraction (if any) of infinite strings [11]. However, as seen from the fact that the above mentioned studies were carried out exclusively by the Monte-Carlo simulations, little work on the dynamical aspects of string formation has been done.

One exception is Borrill's paper [12], where the simulation of the bubble nucleation process in a first order phase transition is performed using a lattice-free method. However, in his approach the subsequent evolution of the string network could not be followed. In Ref. [13] the Langevin-equation approach is considered. But in that study the effect of the expansion of the universe was considered only partially. This is quite different from the real dynamics. Ye and Brandenberger [14], on the other hand, performed a numerical simulation properly taking cosmic expansion into account. But there, a Mexican-hat potential was adopted from the outset, and the simulation domain was so small that the whole system fell within one horizon before they could conclude that the network had reached the scaling regime. The evolution of local (gauged) strings has been investigated by using the Nambu-Goto action. There are many analytical [15] and numerical [16] approaches, and it has been confirmed that the string networks relax to the scaling solution by intercommutation which generates closed loops that eventually disappear by radiating gravitational waves or particles. On the other hand, as for global strings, the Kalb-Ramond action [17] must be used instead of the Nambu-goto action in order to examine the evolution. But in that approach it is difficult to include the long-range force between infinite strings. Here, we use an approach based on a complex scalar field.

In this paper, we simulate both the formation and evolution of the global string network by solving the dynamics of the complex scalar field directly. Starting from a symmetry-restored stage, we follow the dynamics of the complex scalar field, fully considering the expansion of the universe and the associated change of the effective potential, which exhibits spontaneous symmetry breaking below the critical temperature.

The simulation is made in 2+1 dimensions as a first step to analyze the full 3+1-

dimensional analysis, because the spatial resolution and total cosmic time are limited due to our limited computing power. Note that in 2+1 dimensions strings are point-like, and each such string corresponds to an infinite string in 3+1 dimensions so that the energy loss mechanism is pair-annihilation rather than loop-formation through intercommutation. The direct emission of goldstone modes from strings is suppressed because of the symmetry of the system. In a forth-coming paper we will report the results of our simulations in 3+1 dimensions and their cosmological implications [18].

The remainder of this paper is organized as follows. In the next section, we establish the formulation for the numerical simulation. In §3, we give the result of the numerical simulation and judge whether during the evolution the scaling behavior is observed as expected from the analogy of local strings. In §4, the results obtained from the simulation are explained analytically using a phenomenological model. Finally, §5 is devoted to summary and discussion.

2 Formulation

We consider the following Lagrangian density for a complex scalar field $\Phi(x)$:

$$\mathcal{L}[\Phi] = \partial_\mu \Phi \partial^\mu \Phi^\dagger - V[\Phi]. \quad (1)$$

Here, the potential $V[\Phi]$ is given by

$$V[\Phi] = \frac{\lambda}{2} (\Phi \Phi^\dagger - \eta^2)^2. \quad (2)$$

Then the one-loop finite temperature effective potential $V_{\text{eff}}[\Phi]$ in the high temperature limit is written as

$$V_{\text{eff}}[\Phi] = \frac{\lambda}{2} (\Phi \Phi^\dagger - \eta^2)^2 + \frac{\lambda}{3} T^2 \Phi \Phi^\dagger. \quad (3)$$

For $T > T_c = \sqrt{3}\eta$, the potential V_{eff} has a minimum at $\Phi = 0$, and the $U(1)$ symmetry is restored. On the other hand, new minima $|\Phi|_{\text{min}} = \eta \sqrt{1 - (T/T_c)^2}$ appear and the symmetry is broken for $T < T_c$ (Fig. 1). In this case the phase transition is of second order.

In the expanding universe the effective Lagrangian density $\mathcal{L}_{\text{eff}}[\Phi]$ is given by

$$\mathcal{L}_{\text{eff}}[\Phi] = g_{\mu\nu} (\partial^\mu \Phi) (\partial^\nu \Phi)^\dagger - V_{\text{eff}}[\Phi], \quad (4)$$

where $g_{\mu\nu}$ is identified with the Robertson-Walker metric. Then the equation of motion is

$$\ddot{\Phi}(x) + 3H\dot{\Phi}(x) - \frac{1}{a(t)^2} \nabla^2 \Phi(x) = -V'_{\text{eff}}[\Phi], \quad (5)$$

where the prime represents the derivative $\partial/\partial\Phi^\dagger$, and $a(t)$ is a scale factor. The Hubble parameter $H = \dot{a}(t)/a(t)$ and the cosmic time t are given by

$$H^2 = \frac{8\pi}{3M_{\text{pl}}^2} \frac{\pi^2}{30} g_* T^4, \quad t = \frac{1}{2H} = \frac{\xi}{T^2}, \quad (6)$$

where M_{pl} is the Plank mass, g_* is the total number of degrees of freedom for the relativistic particles, and radiation domination is assumed. We define the dimensionless parameter ζ as

$$\zeta \equiv \frac{\xi}{\eta} = \left(\frac{45M_{\text{pl}}^2}{16\pi^3 g_* \eta^2} \right)^{1/2}. \quad (7)$$

In our simulation, we take $\zeta = 10$, which corresponds to $\eta \sim (10^{15} - 10^{16})$ GeV, but the essential result is independent of this choice. The energy density of each point is written as

$$\rho(x) = \dot{\Phi}(x)\dot{\Phi}^\dagger(x) + \frac{1}{a(t)^2} \nabla\Phi(x) \cdot \nabla\Phi^\dagger(x) + V_{\text{eff}}[\Phi]. \quad (8)$$

We simulate the system in 2+1 dimensions from the initial time $t_i = t_c/4$, that is, $T_i = 2T_c$, to the final time $t_f = 150t_i = 37.5t_c$, when $T_f \sim T_c/6.1$. Since the $U(1)$ symmetry is restored at the initial time $t = t_i$, we adopt as the initial condition the thermal equilibrium state with the mass squared,

$$m^2 = \left. \frac{d^2 V_{\text{eff}}[|\Phi|]}{d|\Phi|^2} \right|_{|\Phi|=0}, \quad (9)$$

which is the inverse curvature of the potential at the origin at $t = t_i$. In the thermal equilibrium state, Φ and $\dot{\Phi}$ are Gaussian distributed with the correlation functions,

$$\langle \beta |\Phi(\mathbf{x})\Phi^\dagger(\mathbf{y})| \beta \rangle_{\text{equal-time}} = \int \frac{d\mathbf{k}}{(2\pi)^3} \frac{1}{2\sqrt{\mathbf{k}^2 + m^2}} \coth \frac{\beta\sqrt{\mathbf{k}^2 + m^2}}{2} e^{i\mathbf{k}\cdot(\mathbf{x}-\mathbf{y})}, \quad (10)$$

$$\langle \beta |\dot{\Phi}(\mathbf{x})\dot{\Phi}^\dagger(\mathbf{y})| \beta \rangle_{\text{equal-time}} = \int \frac{d\mathbf{k}}{(2\pi)^3} \frac{\sqrt{\mathbf{k}^2 + m^2}}{2} \coth \frac{\beta\sqrt{\mathbf{k}^2 + m^2}}{2} e^{i\mathbf{k}\cdot(\mathbf{x}-\mathbf{y})}. \quad (11)$$

The functions $\Phi(\mathbf{x})$ and $\dot{\Phi}(\mathbf{y})$ are uncorrelated for $\mathbf{x} \neq \mathbf{y}$. We generate these fields for the initial condition in the momentum space, because the corresponding fields $\tilde{\Phi}(\mathbf{k})$ and $\tilde{\dot{\Phi}}(\mathbf{k})$ are uncorrelated there.

Hereafter we measure the scalar field in units of t_i^{-1} , t and x in units of t_i , and the energy density in units of t_i^{-4} . The equation of motion and the total energy density are given by

$$\ddot{\Phi}(x) + \frac{3}{2t}\dot{\Phi}(x) - \frac{1}{t}\nabla^2\Phi(x) = - \left(|\Phi|^2 + \frac{25}{9t} - \frac{25}{36} \right) \Phi^\dagger, \quad (12)$$

$$\rho(x) = \dot{\Phi}(x)\dot{\Phi}^\dagger(x) + \frac{1}{t}\nabla\Phi(x) \cdot \nabla\Phi^\dagger(x) + \frac{1}{2} \left(|\Phi|^2 - \frac{25}{36} \right)^2 + \frac{25}{9t}|\Phi|^2, \quad (13)$$

where λ is set to unity.¹ The scale factor $a(t)$ is normalized as $a(1) = 1$. We arrange 512×512 lattice points for our simulations. The lattice spacing δx is set to 0.1, and its

¹Strictly speaking, the high temperature approximation is valid only when λ is much smaller than unity. However, a change of λ only scales the physical quantity and is not relevant to the final result.

physical length δx_{phys} grows as $a(t)\delta x = 0.1 t^{1/2}$. The time step δt is chosen to be 0.01. At sufficiently low temperatures, the typical width of the string d is nearly $1/\eta$. Then,

$$\frac{H^{-1}}{\delta x_{\text{phys}}} = 20 t^{1/2}, \quad (\sim 245 \text{ at } t = t_f) \quad (14)$$

$$\frac{d}{\delta x_{\text{phys}}} = 12 t^{-1/2}. \quad (\sim 0.98 \text{ at } t = t_f) \quad (15)$$

Even at the final time t_f , the resolution of the simulation is sufficiently good, and the simulation box is larger than the horizon scale, so that we can safely impose a periodic boundary condition.

Under these circumstances, we simulated the system using the second order leap-frog method and the Crank-Nicholson scheme over 100 runs with a different random realization of the initial conditions.

3 Results

First we depict in Figs. 2~5 how strings are generated as the symmetry is spontaneously broken and the gradient and kinetic energy density decreases. In these figures, the total energy density at each lattice point is depicted at $t = 1, 50, 100, 150$. One can see that initially the field fluctuates very strongly and the gradient and kinetic energy dominates over the potential energy. But as the universe expands and the temperature decreases, the false vacuum energy becomes dominant, and the string configurations become stable.

Next, in order to judge whether the string network really enters a scaling regime in this case, we count the number of strings per horizon volume at various times. Since spacetime is discretized in our simulations, a point at which $\Phi = 0$ corresponding to a string core is not necessarily situated at a lattice point. In the worst case, a point at which $\Phi = 0$ lies at the center of a plaquette. Therefore in order to identify a string, we stipulate that a lattice is identified with a part of a string if the potential energy density there is larger than that corresponding to the field value of a static string solution at $r = \delta x_{\text{phys}}/\sqrt{2}$,² which is obtained by solving the equation

$$\frac{\partial^2 \rho}{\partial r^2} + \frac{1}{r} \frac{\partial \rho}{\partial r} - \frac{\rho}{r^2} - V'_{\text{eff}}[\rho] = 0, \quad (16)$$

with $\Phi(r, \theta) \equiv \rho(r)e^{i\theta}$. Then we regard a connected region of lattices satisfying the above condition as one string. Around $t = 20$, the kinetic and the gradient energy is sufficiently suppressed in comparison with the vacuum energy of the string so that we can identify the string unambiguously. We carried out this identification procedure every 10 steps after $t = 20$.

Figure 6 displays that time evolution of the number of strings per horizon volume averaged over 100 realizations. It is clear that the number is not constant but gradually increases with the cosmic time. Since the rate of increase is a decreasing function of time, one may think that we have observed only a relaxation stage and that it will

²In fact, the potential energy is peaked so highly at the string that the identification of the string depends very little on this criterion.

eventually approach a constant. In order to judge if this is the case, we run a different set of simulations with different initial conditions, in which strings and anti-strings are arranged by turns every two lattices, like a checker-board, and $\dot{\Phi}$ is set to 0 for all lattices. The initial string number per horizon volume in this case is as large as 100. The result is depicted in Fig. 7 together with the previous result. The number per horizon volume rapidly decreases once and then rebounds and continues to increase, as in the previous case. This result implies that the upward trend in the previous simulation is genuine, because, if it were spurious, it would gradually decrease and approach the asymptotic constant value from above. In the next section we present a phenomenological analytic model to explain why a departure from the scaling solution is obtained.

4 Analytic explanation

In the present simulations in 2+1 dimensions, strings are represented by point-like quasi-particles and anti-particles depending on the direction of the winding. Here, strings cannot intercommute with each other to form loops, but rather they can only pair-annihilate upon collision. Between a string and an anti-string works an attractive force proportional to the inverse separation, which is a consequence of the extended field gradient as a global defect. Seen from the simulation result, as the system relaxes sufficiently and enters a quasi-equilibrium state, a string usually remains at rest because it loses kinetic energy due to cosmic expansion. Once within the horizon, a pair of strings feel the above long-range force, and they start moving toward each other. Therefore, we have only to elucidate the dynamics of a pair of particles obeying such a force in an expanding universe.

Let $n(t)$ be the average number of strings per unit physical volume at the cosmic time t . When the system is in a quasi-equilibrium state, the probability per unit time $P(t)$ that a string annihilates with an anti-string is written by

$$P(t) \sim \frac{1}{T(t)}, \quad (17)$$

where $T(t)$ is the period required for a pair of strings at rest with mean separation, $\sim 1/n(t)$, to pair-annihilate. Since $n(t)$ is diluted by cosmic expansion and the above annihilation process, it satisfies the Boltzmann equation,

$$\begin{aligned} \frac{dn(t)}{dt} &= -P(t)n(t) - 2Hn(t), \\ &= -\frac{n(t)}{T(t)} - \frac{n(t)}{t}. \end{aligned} \quad (18)$$

In order to determine the time dependence of $T(t)$, we investigate the relative motion of particles subject to an attractive force proportional to the inverse separation in an expanding universe, which is described by the equation

$$\frac{d^2r}{dt^2} + \frac{1}{t} \frac{dr}{dt} = -\frac{2\pi}{a(t)^2 r}, \quad (19)$$

where r is the comoving separation. In terms of the physical separation $x \equiv a(t)r = (t/t_i)^{1/2}r$, this equation reads

$$\frac{d^2x}{dt^2} + \frac{1}{4t^2}x = -\frac{2\pi}{x}. \quad (20)$$

For the moment, we neglect the dissipation term due to cosmic expansion. This is justified below. Then integration of Eq. (20) over t gives

$$\frac{1}{2} \left(\frac{dx}{dt} \right)^2 + 2\pi \ln \left(\frac{x}{x_0} \right) = 0, \quad (21)$$

where $\frac{dx}{dt} = 0$ and $x = x_0$ at $t = 0$. Then the period T is estimated as

$$\begin{aligned} T &= \int_0^T dt = \int_{x_0}^d \frac{-dx}{\sqrt{-4\pi \ln \left(\frac{x}{x_0} \right)}} \\ &= \frac{1}{2\sqrt{\pi}} \left\{ \left[-2x \sqrt{\ln \left(\frac{x_0}{x} \right)} \right]_d^{x_0} + 2 \int_d^{x_0} \sqrt{\ln \left(\frac{x_0}{x} \right)} dx \right\} \\ &\sim \sqrt{\frac{1}{\pi}} x_0 \sqrt{\ln \left(\frac{x_0}{d} \right)}, \end{aligned} \quad (22)$$

where d is the core radius. Before inserting this into Eq. (18) to solve for $n(t)$, we justify the omission of the dissipation term. A pair of strings at rest initially with separation x_0 approach a separation x in a time interval t given by

$$t \sim \sqrt{\frac{1}{\pi}} x_0 \sqrt{\ln \left(\frac{x_0}{x} \right)}. \quad (23)$$

Then the dissipation term, $x/(4t^2)$, reads $\pi x/(4x_0^2 \ln(x_0/x))$. Since x is smaller than x_0 , the term from the potential force in Eq. (20), $2\pi/x$, always dominates over the dissipation term.

Taking x_0 as the mean separation, $1/\sqrt{n(t)}$, Eq. (18) becomes

$$\begin{aligned} \frac{dn(t)}{dt} &= -\frac{\sqrt{\pi} n(t)^{\frac{3}{2}}}{\sqrt{\ln \left(\frac{1}{d\sqrt{n(t)}} \right)}} - \frac{n(t)}{t} \\ &\sim -\frac{\sqrt{\pi} n(t)^{\frac{3}{2}}}{\sqrt{\ln \left(\frac{At}{d} \right)}} - \frac{n(t)}{t}, \end{aligned} \quad (24)$$

where $1/\sqrt{n(t)}$ is nearly proportional to the cosmic time from the simulation result, and the proportional coefficient is A . Substituting $f(t)$ for $n(t)t$, we have

$$\frac{1}{t} \frac{df}{dt} = -\frac{\sqrt{\pi} f^{3/2}}{\sqrt{\ln \left(\frac{At}{d} \right)}} \frac{1}{t^{3/2}}. \quad (25)$$

Integrating over both sides gives

$$\frac{1}{f^{1/2}} \sim \sqrt{\pi} B \frac{t^{1/2}}{\sqrt{\ln \left(\frac{At}{d} \right)}} + C, \quad (26)$$

where B represents a numerical factor $\sim \mathcal{O}(1)$ and C is an integration constant determined from the initial conditions.

Then $n(t)$ is given by

$$n(t) \sim \frac{D}{t^2} \frac{\ln\left(\frac{t}{E}\right)}{\left[1 + \frac{CD^{1/2}}{t^{1/2}} \sqrt{\ln\left(\frac{t}{E}\right)}\right]^2}, \quad (27)$$

where $D = (\pi B^2)^{-1}$, $E \sim d/A \sim d/\sqrt{D}$. Therefore the number of strings per horizon volume is given by

$$\begin{aligned} n(t)H^{-2} &\sim 4D \frac{\ln\left(\frac{t}{E}\right)}{\left[1 + \frac{CD^{1/2}}{t^{1/2}} \sqrt{\ln\left(\frac{t}{E}\right)}\right]^2} \\ &\implies 4D \ln\left(\frac{t}{E}\right). \quad (\text{asymptotically}) \end{aligned} \quad (28)$$

Taking $D \sim 0.1$, $E \sim 0.4$ ($d \sim 1.0$) and $C \sim -0.09$, we can fit the results of the simulation by the above formula. This is depicted in Fig. 7. The number of strings per horizon volume is not a constant, but proportional to $(\ln t)$ asymptotically. Note that only the constant C depends on the initial conditions. Taking $C \sim 0.8$ with almost the same D and E , that from the checker-board initial conditions can also be fitted. This implies that our fitting formula is consistent.

5 Summary and Discussion

In this paper, we have reported the dynamics of a complex scalar field from the symmetric phase to the broken phase in 2+1 dimensions. Starting from the thermal equilibrium state, we have observed how strings are formed as the temperature decreases and the symmetry is spontaneously broken. We also find that, as the string system grows, it does not go into a scaling regime, where the number of strings per horizon volume stays constant, but the number increases in proportion to $(\ln t)$ asymptotically. This can be interpreted as follows. Our simulation was performed in 2+1 dimensions and strings are in fact point-like. Thus, the dominant energy loss process is not the formation of loops through the intercommutation of infinite strings, but rather pair-annihilation of straight strings. They move under logarithmic potentials, which causes deviation from scale-invariance.

Acknowledgments

MY is grateful to Professor K. Sato for his continuous encouragement and Dr. T. Shiromizu and Professor M. Morikawa for their useful comments. JY would like to thank Professor Andrei Linde for his hospitality at Stanford University, where part of this work was done. This work was partially supported by the Japanese Grant-in-Aid for Scientific Research from the Monbusho, Nos. 10-04558 (MY), 09740334 (JY) and 10640250 (MK). JY acknowledges support from the Monbusho.

References

- [1] D. A. Kirzhnits and A. D. Linde, Phys. Lett. **B42** (1985), 471.
- [2] For example, see M. Kolb and E. Turner, *The Early Universe* (Addison-Wesley, New York, 1990) and A. D. Linde, *Particle Physics and Inflationary Cosmology* (Harwood, New York, 1990).
- [3] T. W. B. Kibble, J. Phys. **A9** (1976), 1387.
- [4] A. Vilenkin and E. P. S. Shellard, *Cosmic String and Other Topological Defects* (Cambridge University Press, Cambridge, 1994). A. Vilenkin, Phys. Rep. **121** (1985), 263. M. Hindmarsh and T. W. B. Kibble, Rep. Prog. Phys. **58** (1994), 477.
- [5] R. Brandenberger, “Formation of Structure in the Universe” in *the proc. of the VIIIth Brazilian School of Cosmology*, ed. M. Novello (Editions Frontières, Paris, 1996).
- [6] R. D. Peccei and H. R. Quinn, Phys. Rev. Lett **38** (1977), 1440.
- [7] R. Davis, Phys. Lett. **B180** (1986), 225. M. Nagasawa and M. Kawasaki, Phys. Rev. **D50** (1994), 4821.
- [8] I. Chuang, R. Durrer, N. Turok, and B. Yurke, Science **251** (1996), 1336. W. H. Zurek, Phys. Rep. **276** (1996), 177.
- [9] T. Vachaspati and A. Vilenkin, Phys. Rev. **D30** (1984), 2036.
- [10] R. J. Scherrer and J. Frieman, Phys. Rev. **D33** (1986), 3556.
- [11] H. M. Hodges, Phys. Rev. **D40** (1989), 1798. T. Vachaspati, Phys. Rev. **D44** (1991), 3723. A. Yate and T. W. B. Kibble, Phys. Lett. **B364** (1995), 149. M. Hindmarsh and K. Strobl, Nucl. Phys. **B347** (1995), 471. J. Robinson and A. Yates Phys. Rev. **D54** (1996), 5211. R. J. Scherrer and A. Vilenkin, Phys. Rev. **D56** (1997), 647.
- [12] J. Borrill, Phys. Rev. Lett **76** (1996), 3255.
- [13] H. M. Hodges, Phys. Rev. **D39** (1989), 3557.
- [14] J. Ye and R. Brandenberger, Mod. Phys. Lett. **A5** (1990), 157; Nucl. Phys. **B346** (1990), 149.
- [15] T. W. B. Kibble, Nucl. Phys. **B252** (1985), 227. D. P. Bennett, Phys. Rev. **D33** (1986), 872; **D34** (1986), 3592. D. Austion, E. J. Copeland, and T. W. B. Kibble, Phys. Rev. **D48** (1993), 5594. M. Hindmarsh, Phys. Rev. Lett. **77** (1996), 4495. C. J. A. P. Martins and E. P. S. Shellard, Phys. Rev. **D54** (1996), 2535.
- [16] A. Albrecht and N. Turok, Phys. Rev. **D40** (1989), 973. D. P. Bennett and F. R. Bouchet, Phys. Rev. Lett. **60** (1988), 257; **63** (1989), 2776. B. Allen and E. P. S. Shellard, Phys. Rev. Lett. **64** (1990), 119. G. R. Vincent, M. Hindmarsh, and M. Sakellariadou, Phys. Rev. **D56** (1997), 637.

- [17] M. Kalb and P. Ramond Phys. Rev. **D9** (1974), 2273. F. Lund and T. Regge, Phys. Rev. **D14** (1976), 1524.
- [18] M. Yamaguchi, M. Kawasaki and J. Yokoyama, in preparation.

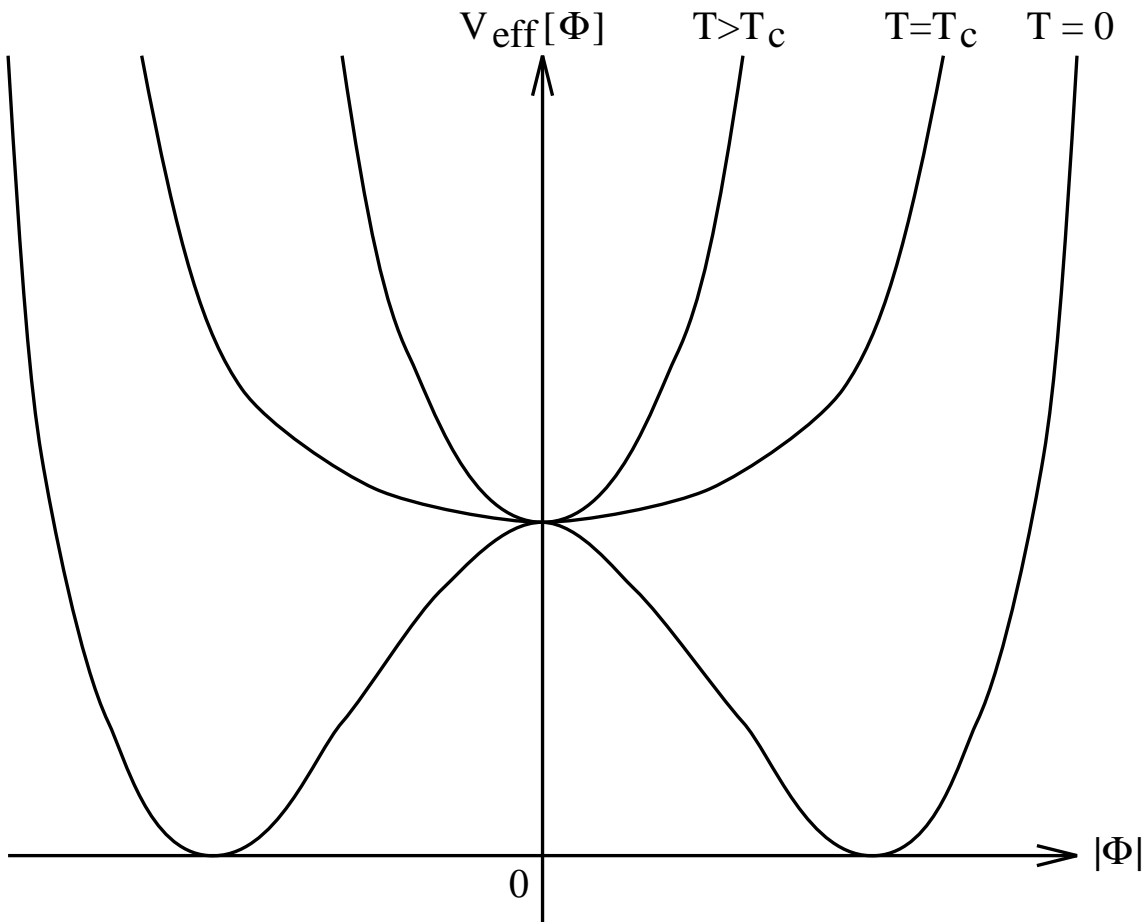


Figure 1: One-loop finite temperature effective potential $V_{\text{eff}}[\Phi]$ of the complex scalar field.

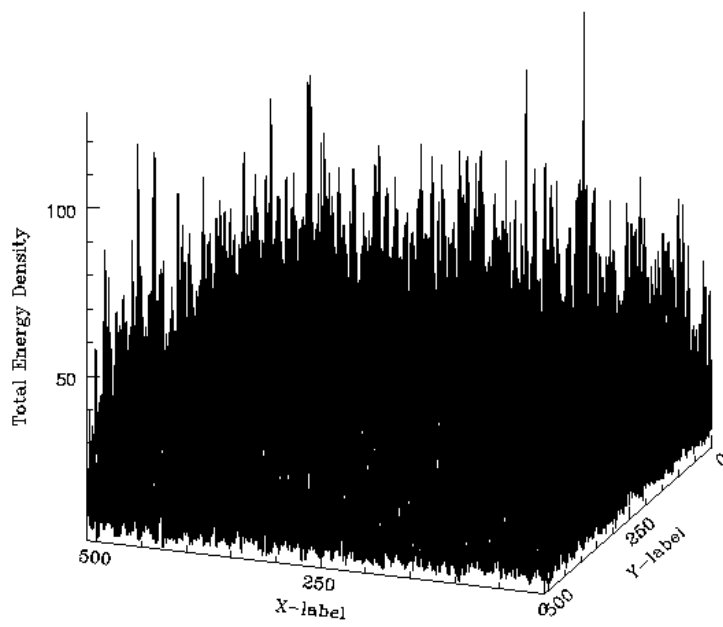


Figure 2: The total energy density for each lattice point is depicted at $t = t_i = 1$.

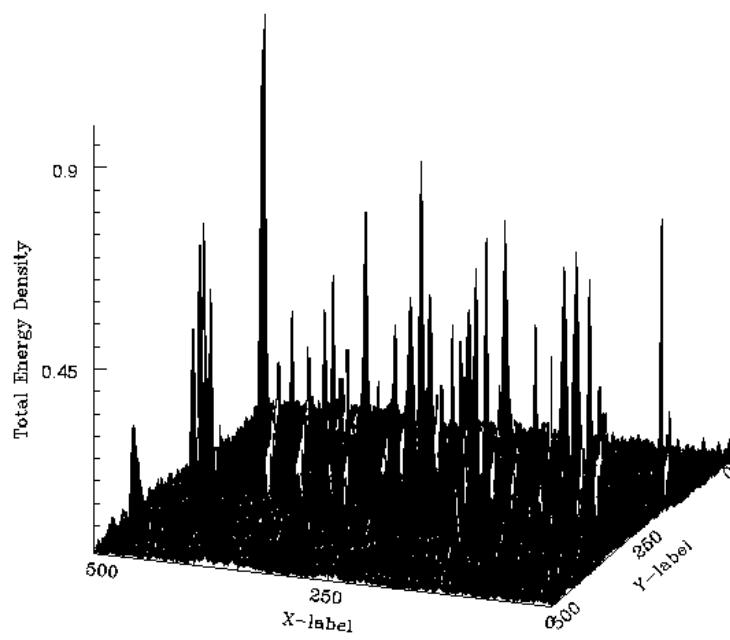


Figure 3: That at $t = 50$.

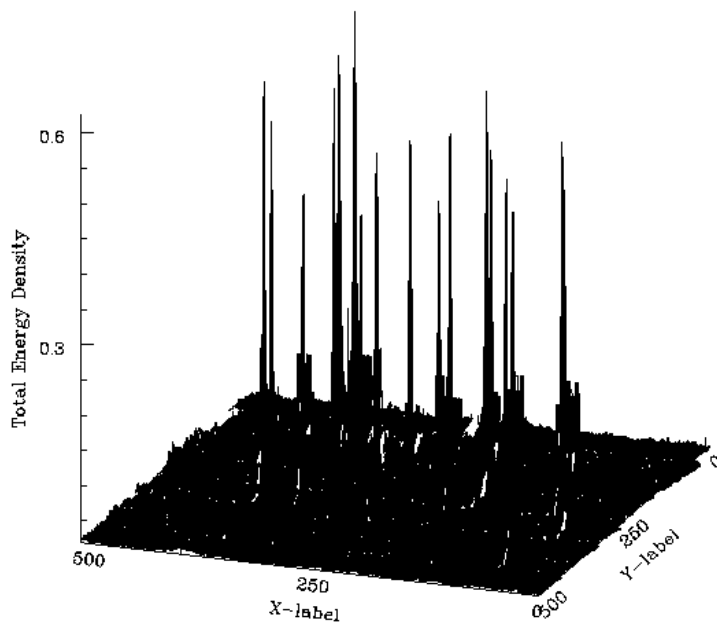


Figure 4: That at $t = 100$.

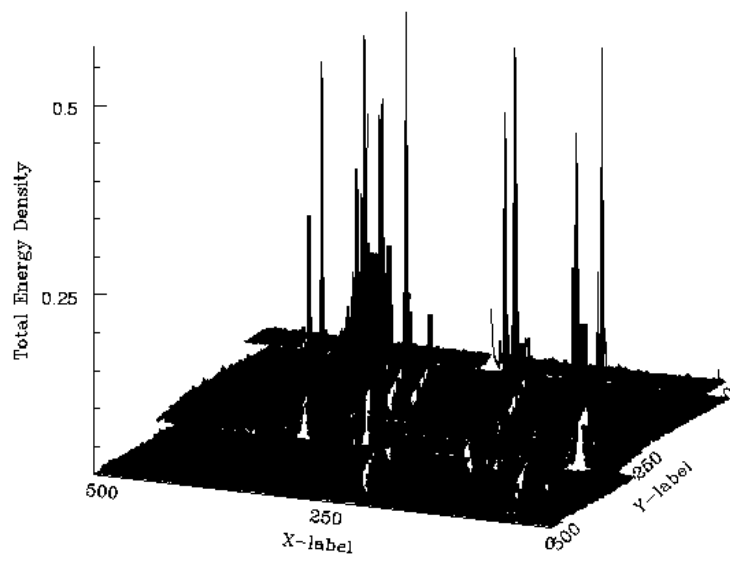


Figure 5: That at $t = 150$.

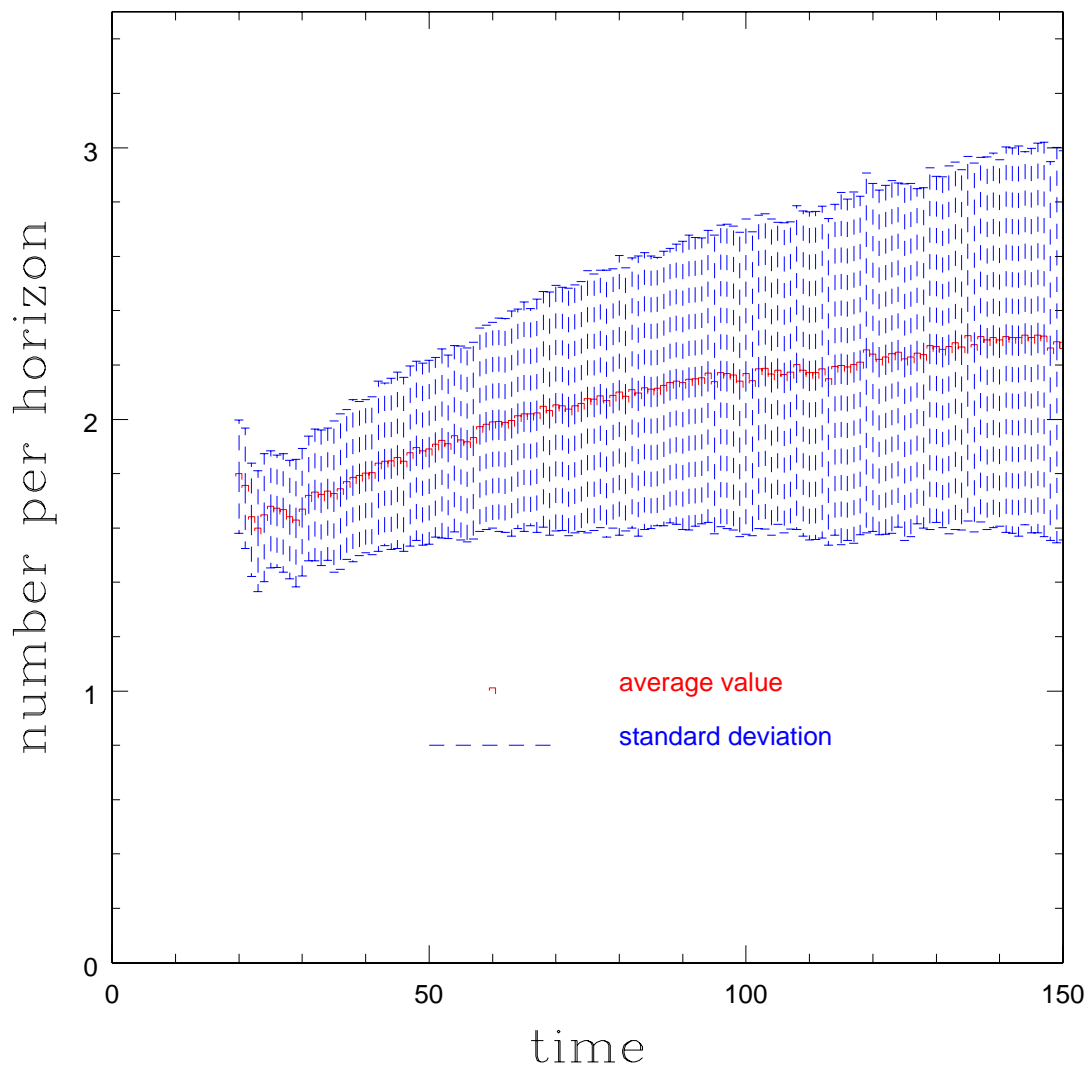


Figure 6: The number of strings per horizon volume is depicted. Dots represent the average value over 100 realizations. Error-bars the standard deviation.

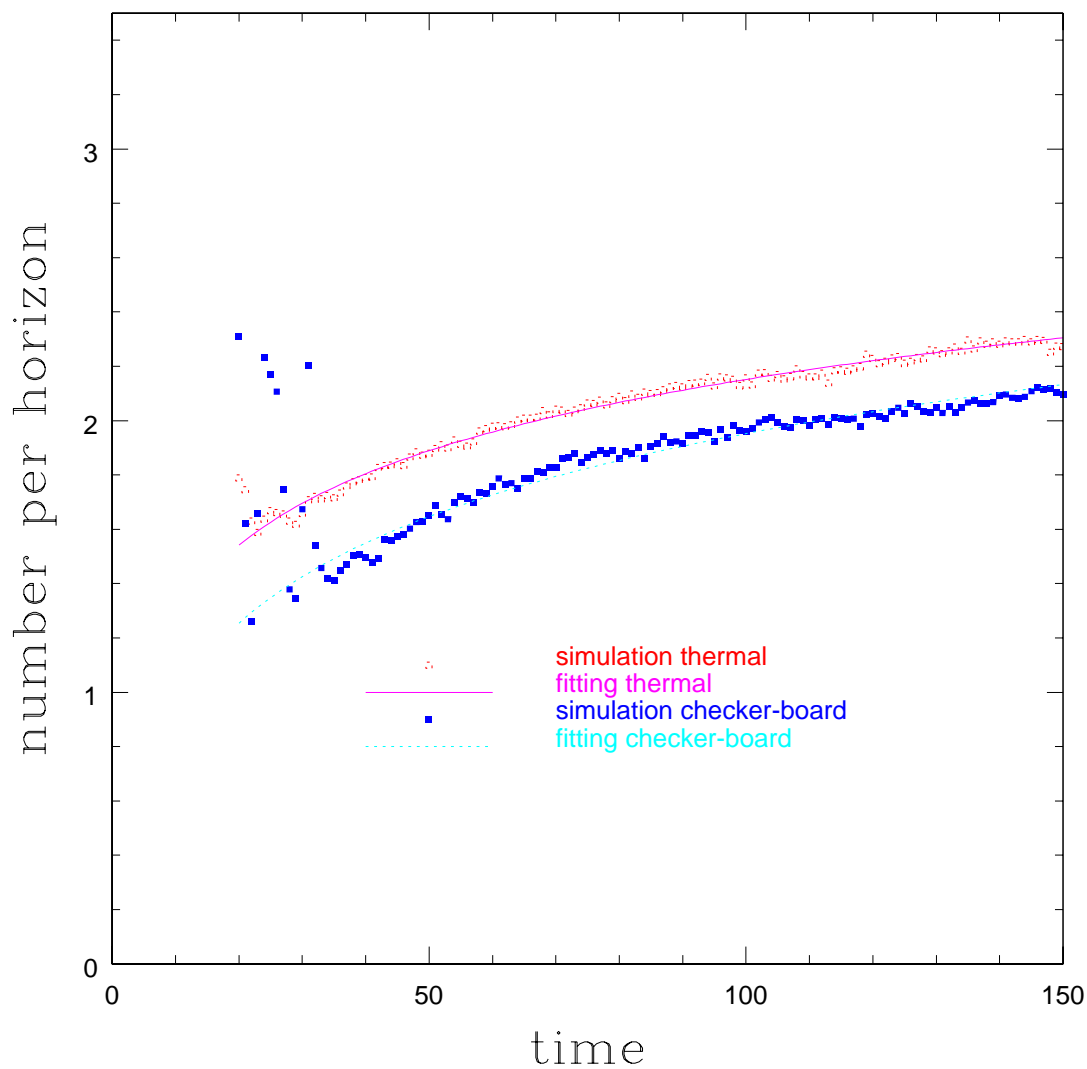


Figure 7: Open dots represent the number of strings per horizon volume averaged over those from 100 initial conditions which are the thermal equilibrium states. On the other hand, filled dots from checker-board initial conditions. Also, a solid line represents the fitting formula for simulation results from thermal initial conditions and a dotted line from checker-board ones.